Biophysical Journal, Volume 97

Supporting Material

Misfolded Amyloid Ion Channels Present Mobile ¥â-Sheet Subunits in Contrast to Conventional Ion Channels

Hyunbum Jang, Fernando Teran Arce, Ricardo Capone, Srinivasan Ramachandran, Ratnesh Lal, and Ruth Nussinov

Supporting Material

Supplementary Document S1

Potential of mean force (PMF) calculations

In order to see the ions' behavior in the pore, the potential of mean force (PMF) representing the relative free energy profile for each ion across the bilayer is calculated. The PMF is calculated by using the equation of $\Delta G_{\mathrm{PMF}} = -k_{\mathrm{B}}T \ln\left(\rho_z / \rho_{\mathrm{bulk}}\right)$. Here, k_{B} is the Boltzmann constant, T is the simulation temperature, ρ_z is the ion density at the position z along the pore axis, and ρ_{bulk} is the ion density in the bulk region. Accurate equilibrium PMF relevant to ion permeation should be obtained from free energy calculations with the umbrella sampling method (1). Nevertheless, given the simulation trajectory without additional multiple equilibrium runs for sampling, ion-density-based PMF calculations are useful to estimate rough relative free energy changes for ions, providing an outline for pore ion permeation (2, 3). On the top bilayer surface, the cations interact with the phosphate headgroups at the lipid/water interface. Just below the interface, the negatively charged Glu^{22} side-chains in the pore form cation binding sites. At the lower bilayer leaflet, the cations interact with the phosphate headgroups and the Aβ C-termini. Three binding sites for each cation across the bilayer may produce the PMF curve with three minima.

References

1. Allen, T. W., O. S. Andersen, and B. Roux. 2006. Molecular dynamics - potential of mean force calculations as a tool for understanding ion permeation and selectivity in narrow channels. Biophys Chem 124:251-267.
2. de Groot, B. L., and H. Grubmuller. 2001. Water permeation across biological membranes: mechanism and dynamics of aquaporin-1 and GlpF. Science 294:2353-2357.
3. Leontiadou, H., A. E. Mark, and S. J. Marrink. 2007. Ion transport across transmembrane pores. Biophys J 92:4209-4215.

Supplementary Table S1

Channel size	Number of molecules, atoms, and ions in the bilayer system								Simulation parameters		
	Lipid	Water	Mg^{2+}	K^{+}	Ca^{2+}	Zn^{2+}	Cl^{-}	Total atoms	*T* (K)*	*t* (ns)*	# of trajectory
12-mer	200 DOPCs	19,381	6	6	6	6	54	91,917	300	30	1
16-mer	340 DOPCs	31,205	8	8	8	8	72	148,767	300	30	3
20-mer	340 DOPCs	32,479	8	8	8	8	76	154,625	300	30	2
24-mer	340 DOPCs	35,661	8	8	8	8	80	166,207	300	30	2
24-mer	272 POPCs + 68 POPGs	30,978	14	14	14	14	54	150,320	310	30	1
36-mer	500 DOPCs	38,935	10	10	10	10	106	204,239	300	50	1

* *T* denotes the simulation temperature, and *t* denotes the time duration of production run.

Table S1. A summary of initial setup of the unit cell containing annular channel, lipid bilayer, TIP3P waters, and ions.

Supplementary Fig. S1

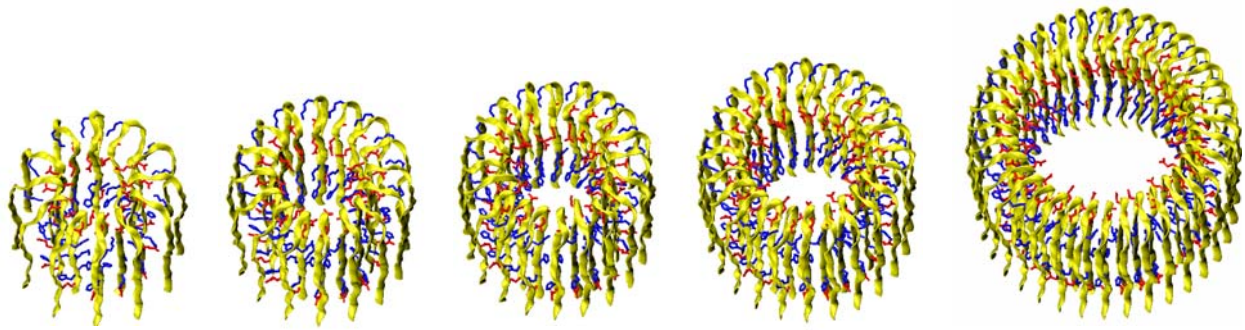

Fig. S1. Building annular channel structures for the 12-, 16-, 20-, 24-, and 36-mer $A\beta_{9-42}$ channels. In the channels, backbone of Aβ peptides is shown in a ribbon representation, and the negatively charged sidechains (Glu^{11}, Glu^{22} and Asp^{23}) and the positively charged sidechains (His^{13}, His^{14}, Lys^{16}, and Lys^{28}) are highlighted by red and blue, respectively.

Supplementary Fig. S2

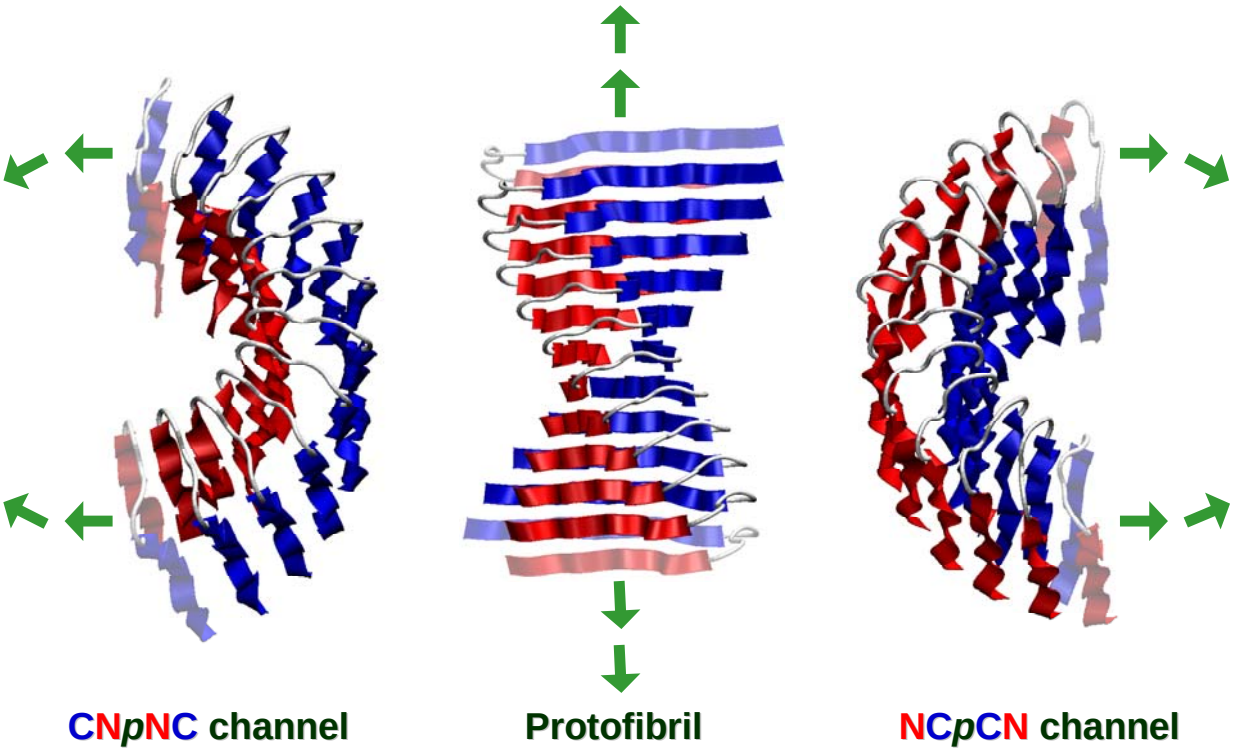

Fig. S2. The figure shows how the initial channel model is constructed using the U-shaped *β-strand-turn-β-strand* motif and the conformation of the channel in the membrane. The NMR based small Aβ oligomer is linearly extended and twisted, yielding a protofibril (center). Two different directions of curvature yield the CN*p*NC (left) and NC*p*CN (right) channels. The arrows indicate the directions of the fibril or channel growth. The peptide backbone is in a ribbon representation; the N-terminal β-strands are shown in red and the C-terminal β-strands are shown in blue. The turns in a tube representation are shown in white.

Supplementary Fig. S3

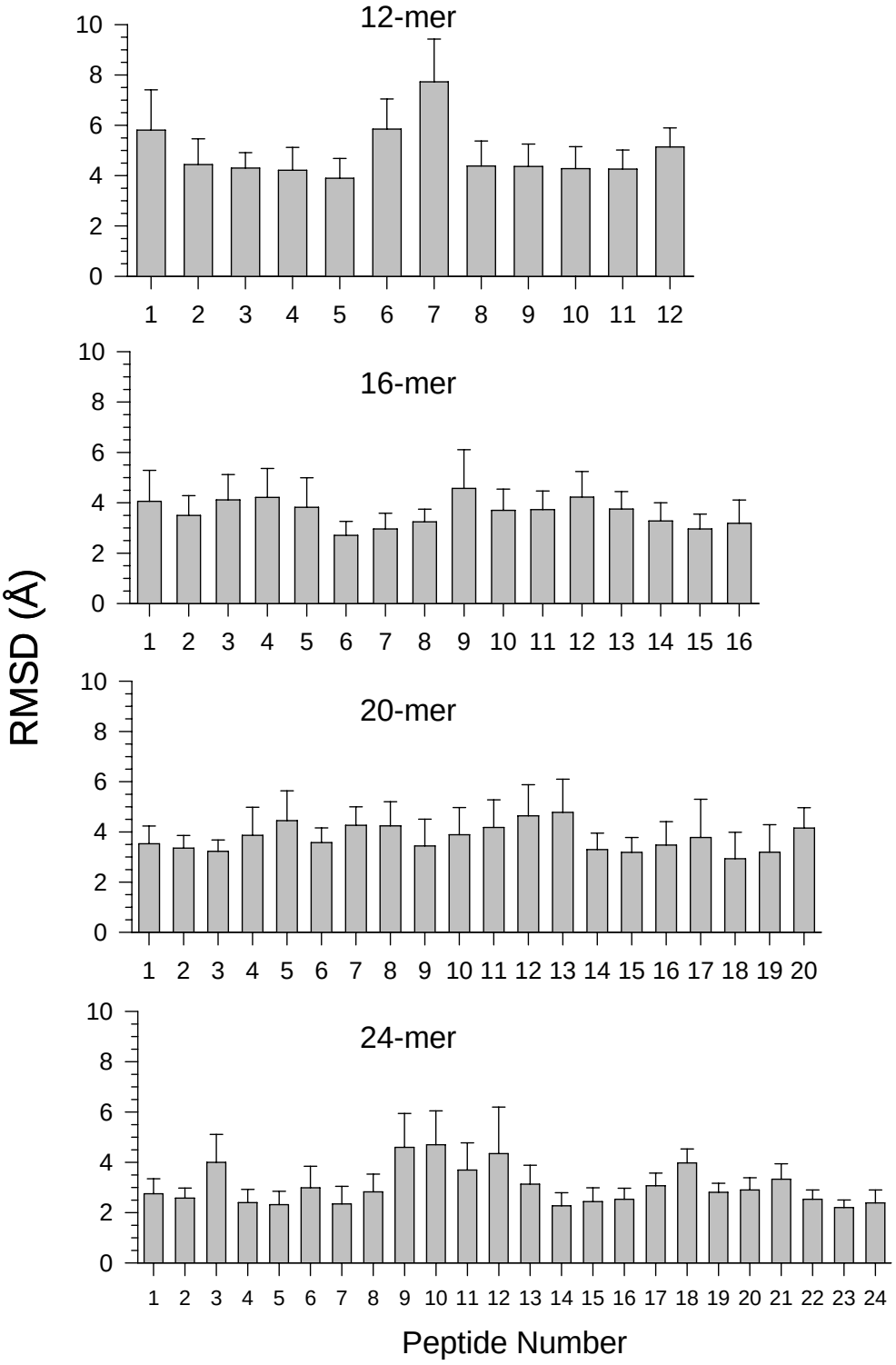

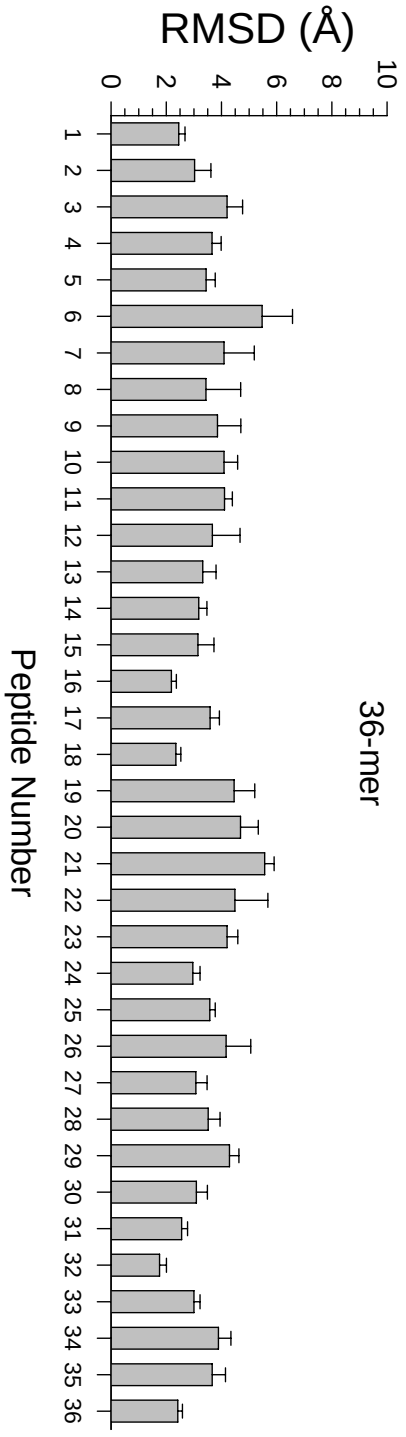

Fig. S3. The average root-mean-squared-deviation (RMSD) from the starting point for backbone atoms of each monomer in the channels. The 12-, 16-, 20-, and 36-mer results were obtained from the simulations in the zwitterionic DOPC bilayer, while the 24-mer results were obtained from the anionic bilayer containing POPC and POPG with a molar ratio of 4:1.

Supplementary Fig. S4

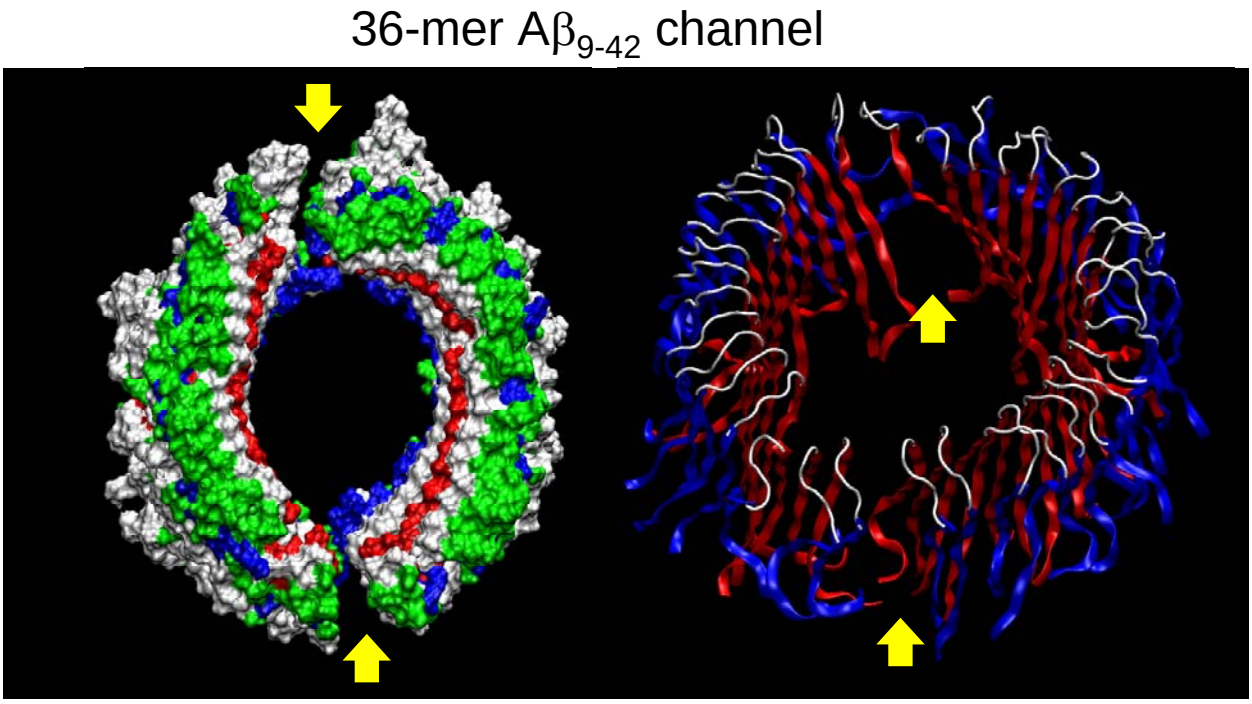

Fig. S4. A snapshot depicted from the final conformation at t = 50 *ns* for the $A\beta_{9\text{-}42}$ 36-mer channel; a top view in a surface representation (left) and an angle view in a ribbon representation (right). An ellipsoidal shape with two broken parts is apparent, suggesting that the lipid bilayer does not support the large pore formation. The channel breakage is highlighted by the yellow arrows. In the surface representation, hydrophobic residues are shown in white, polar and Gly residues are shown in green, positively charged residues are shown in blue, and negatively charged residues are shown in red. The colors used in the ribbon representation are the same as used in Fig. S2.

Supplementary Fig. S5

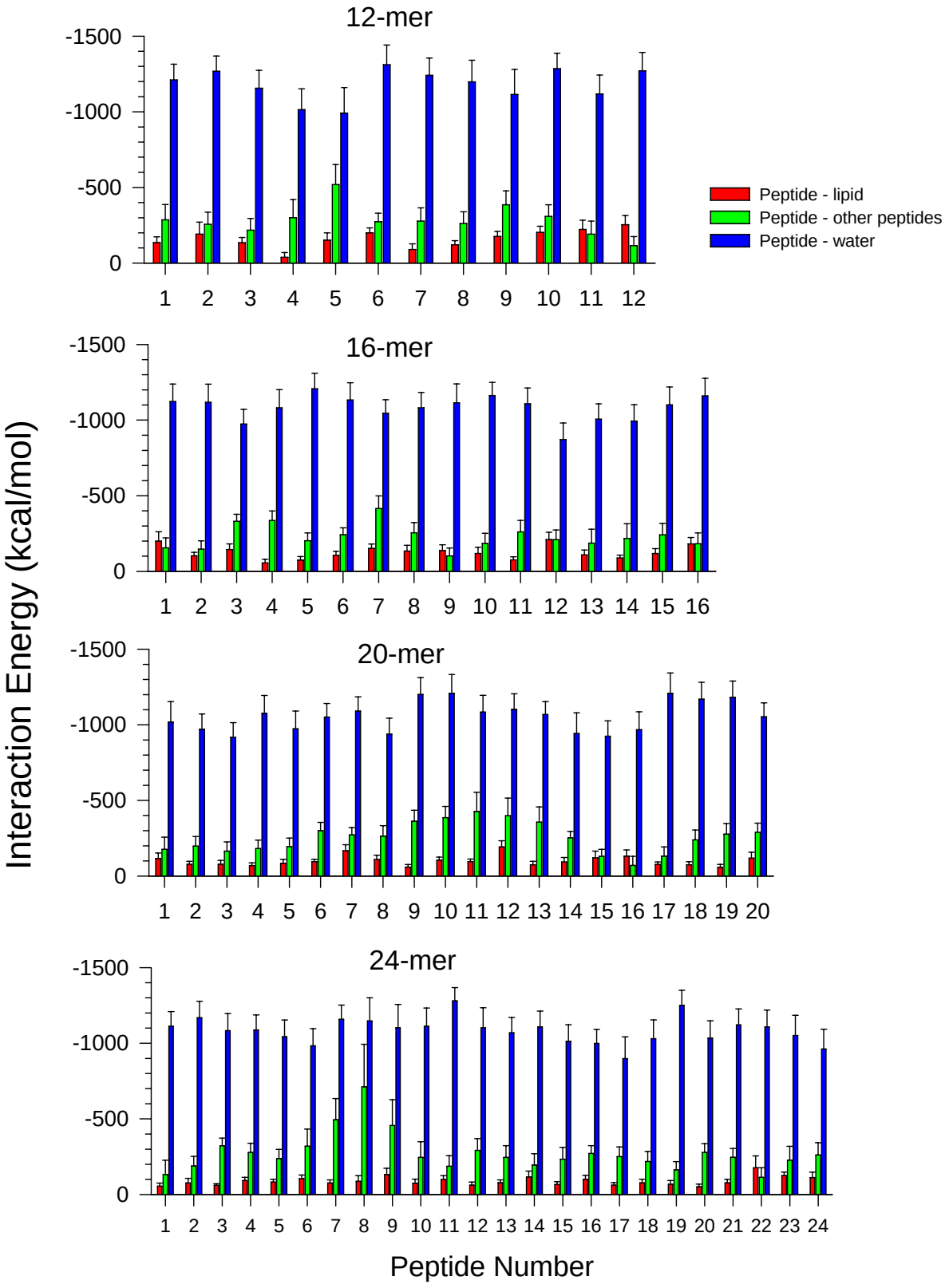

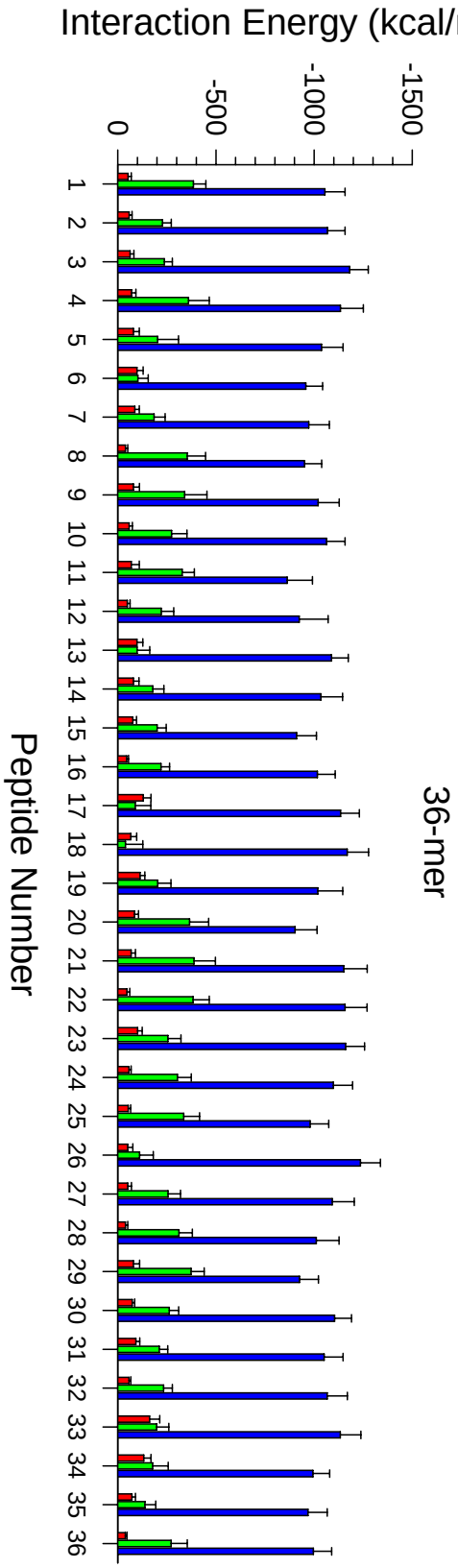

Fig. S5. Interaction energies of each monomer in the Aβ9-42 channels. All peptide-lipid interactions were calculated for the peptides interacting with DOPC lipids including 24-mer channels. Red bars denote the peptide-lipid interaction, green bars denote the peptide-other peptides interaction, and blue bars denote the peptide-water interaction.

Supplementary Fig. S6

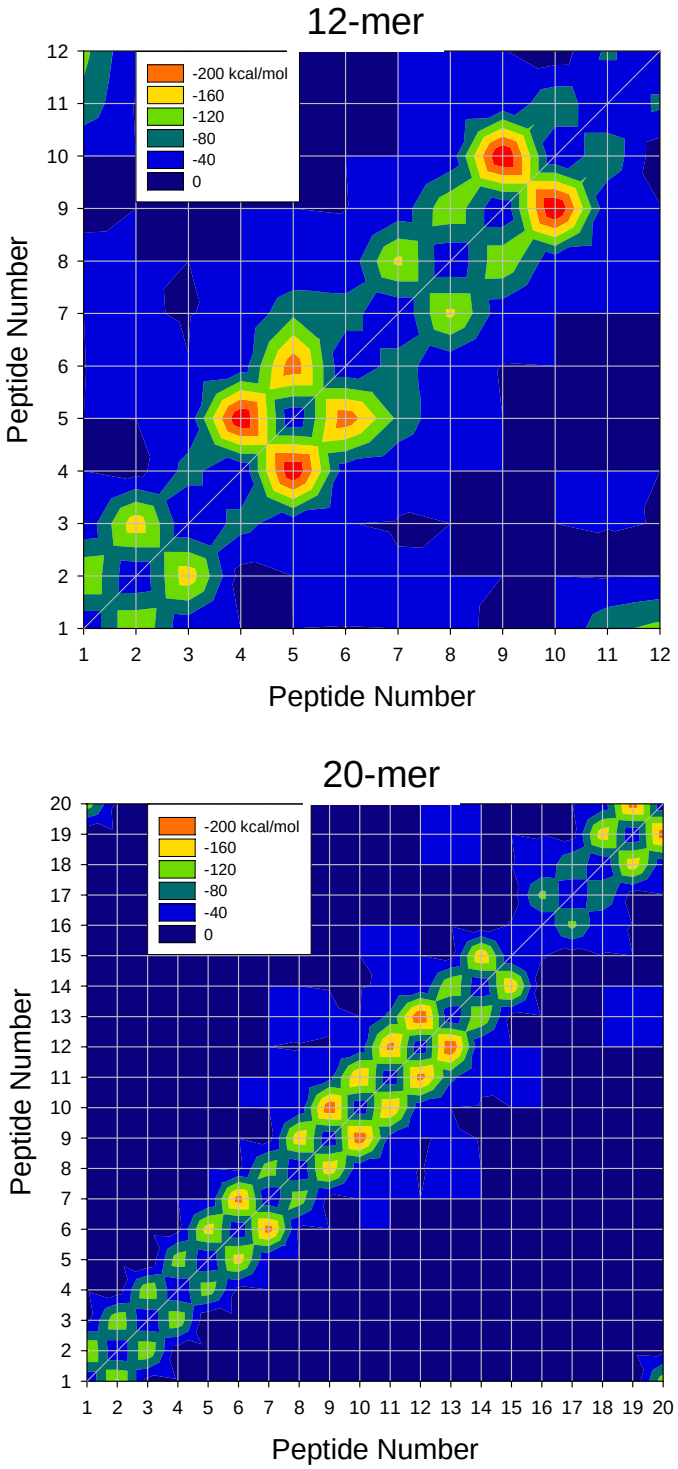

Fig. S6. A contour map representing peptide-peptide interaction energy for the 12-met (upper panel) and 20-mer (lower panel) $A\beta_{9\text{-}42}$ channels.

Supplementary Fig. S7

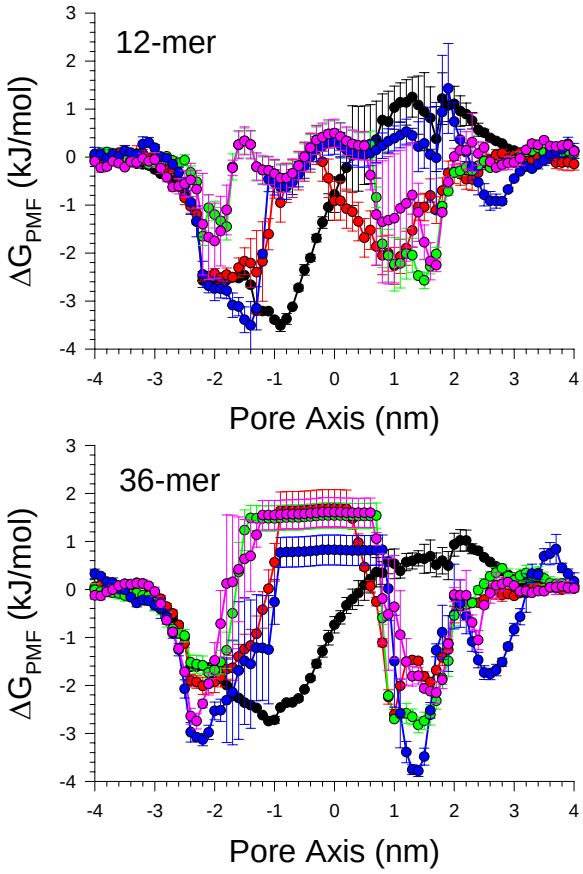

Fig. S7. Potential of mean force (PMF), ΔG_{PMF}, calculated using the equation $\Delta G_{\mathrm{PMF}} = -k_{\mathrm{B}}T \ln(\rho_z/\rho_{\mathrm{bulk}})$, where k_{B} is the Boltzmann constant, T is the simulation temperature, ρ_z is the density of ion at the position z along the pore axis, and ρ_{bulk} is the density of ion in the bulk region, representing the relative free energy profile for Mg^{2+} (green symbols and lines), K^+ (red), Ca^{2+} (blue), Zn^{2+} (pink), and Cl^- (black) as a function of the distance along the pore center axis for the 12-mer (upper panel) and 36-mer (lower panel) $A\beta_{9\text{-}42}$ channels.

Supplementary Fig. S8

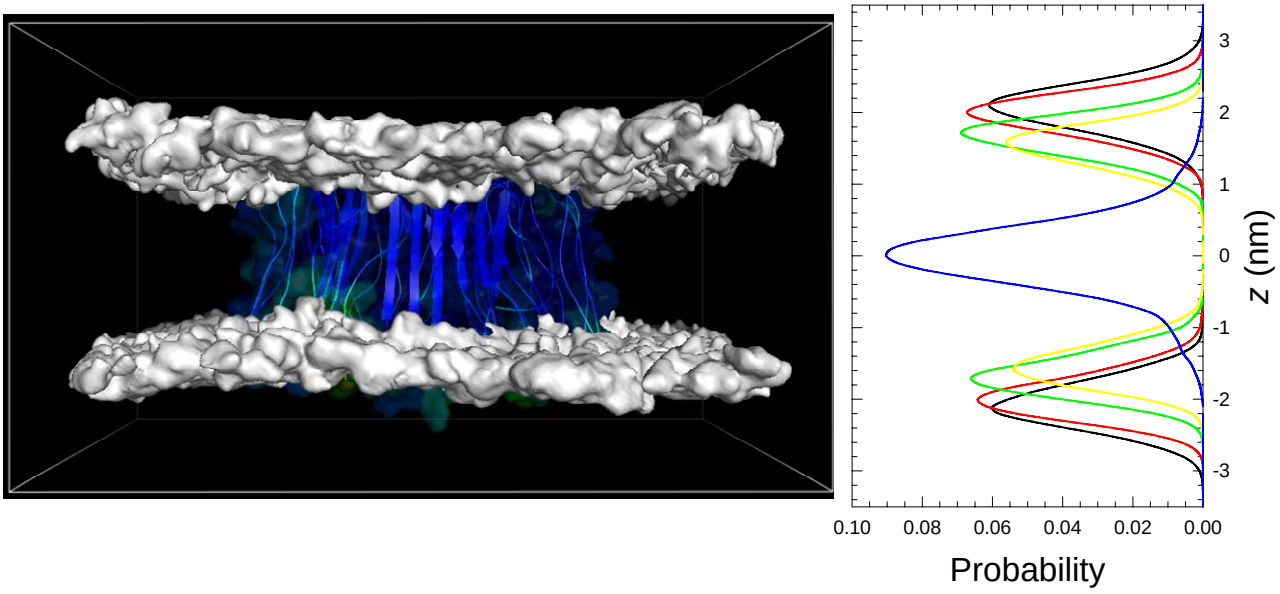

Fig. S8. Three dimensional density maps (left panels) of the lipid headgroup of the DOPC bilayer (white surface) and probability distribution functions (P) (right panels) for different component groups of lipid (P_{Chol} (choline - black lines), P_{PO4} (phosphate - red lines), P_{Glyc} (glycerol - green lines), P_{Carb} (carbonyls - yellow lines), and P_{CH3} (methyl - blue lines)) as a function of the distance along the pore center axis for the 20-mer $A\beta_{9\text{-}42}$ channel. The density maps represent the lateral view of the time averaged bilayer structure. The channel in both surface cartoon representations is embedded in the density maps. The parallel profile of lipid headgroup density map clearly suggests that the $A\beta_{9\text{-}42}$ channel induces the barrel-stave membrane pore. In the barrel-stave pore model a bundle of peptides inserts into the bilayer membrane by placing its hydrophobic portion in contact with the hydrophobic core of the lipid bilayer. The peptide bundle is an ordered aggregate and forms a channel in the membrane pore. No thinning of the bilayer is induced by the channel in the barrel-stave pore model.